Chemistry–A European Journal
Research Article
doi.org/10.1002/chem.202303200
Chemistry Europe
European Chemical Societies Publishing
www.chemeurj.org

Luminescent Chiral Furanol-PAHs via Straightforward Ni-Catalysed C_{sp2}—F Functionalization: Mechanistic Insights into the Scholl Reaction

Judith Sala,[a] Lorena Capdevila,[a] Cristina Berga,[a] Araceli de Aquino,[b] Laura Rodríguez,*[b] Sílvia Simon,*[a] and Xavi Ribas*[a]

Here we report the stepwise synthesis of new nanographenes (NGs) and polycyclic aromatic hydrocarbons (PAHs) obtained via Scholl ring fusion applied at aromatic homologation compounds, which are obtained through one-step Ni-catalysed C_{sp2}—F functionalization. The latter are rapidly accessed valid precursors for the Scholl reaction, and screening of experimental conditions allowed us to describe for the first time furanol-bearing PAHs. Mechanistic insights are obtained by DFT to rationalize the formation of the furanol PAHs under moderately acidic conditions. All PAHs and NGs synthesized show moderate/weak fluorescent properties, and all PAHs crystallized show some degree of curvature and are obtained as racemic mixtures. Enantiomeric separation by chiral HPLC of one furanol-bearing PAH allowed the study of their chiroptical CD properties.

Introduction

Nanographenes (NGs) are gaining relevance as new materials for organic electronics,[1] luminescence[2] and chiroptical applications,[3] among others.[4] NGs are nanoscale polycyclic aromatic hydrocarbons (PAHs) that can be tailored in size, edge-type, non-planarity and chirality,[5] which endows them very rich physical properties, enhanced solubility and specially opening the zero bandgap of the parent 2D graphene. Therefore, their intrinsic semiconducting nature (bandgap >0) is the basis for their optoelectronic properties,[6] which can be implemented in molecular electronics, photovoltaics or sensor applications.[7]

In order to have full control of the size and edge effects of these compounds,[8] tedious bottom-up nanographene precursor synthesis has to be undertaken prior to final ring-fusion graphitization via oxidative cyclodehydrogenation under acidic conditions (Scholl reaction).[9] A large variety of methodologies have been published to reach valid pre-Scholl precursors[9a,10] including cross-coupling reactions,[11] annulative π-extension (APEX),[12] cycloadditions[9a] and cross-cyclotrimerization of arynes (Figure 1).[13]

The latter procedures also include previous multistep synthon synthesis (*ortho* triflate and TMS precursor synthesis, polyaryl cyclopentadienone derivatives, etc.) that complicates enormously the overall nanographene synthesis. Indeed, the final Scholl oxidative ring fusion step is often unpredictable a variety of different conditions have been reported in the recent years.[14] Here we take advantage of a straightforward chemoselective Ni-catalysed C_{sp2}—F activation of readily available substrates bearing the aminoquinoline (AQ) directing group (DG) for the synthesis of aromatic homologation compounds,[15] which are valid precursors for Scholl-like ring fusion (Figure 1).[16]

Moreover, we took these aromatic homologation compounds as basic models and subjected them to a variety of Scholl-type experimental conditions (via oxidant and strong Lewis or Brønsted acid) to obtain a wide array of chiral PAHs as racemates, and we include their photophysical characterization as proof of the rich luminescent properties easily at hand. Remarkably, we report for the first time the synthesis of benzo-chryseno-furanol species, for which we provide full structural, as well as a mechanistic proposal for their formation, obtaining valuable insight into the highly unpredictable Scholl reaction.[17] The chiral HPLC purification of one of them allowed to obtain the CD properties of each enantiomer. Nonetheless, this novel synthetic strategy entails a desirable method for the functionalization of aromatic C_{sp2}—F bonds, as an enabling strategy to

[a] J. Sala, Dr. L. Capdevila, C. Berga, Dr. S. Simon, Prof. X. Ribas
Institut de Química Computacional i Catàlisi (IQCC) and
Departament de Química
Universitat de Girona
Campus Montilivi,17003 Girona, Catalonia (Spain)
E-mail: xavi.ribas@udg.edu
silvia.simon@udg.edu
[b] A. de Aquino, Prof. Dr. L. Rodríguez
Departament de Química Inorgànica i Orgànica
Secció de Química Inorgànica
Universitat de Barcelona
08028 Barcelona (Spain)
Institut de Nanociència i Nanotecnologia (IN2UB)
Universitat de Barcelona
08028 Barcelona, Catalonia (Spain)
E-mail: laurarodriguezr@ub.edu

Supporting information for this article is available on the WWW under https://doi.org/10.1002/chem.202303200

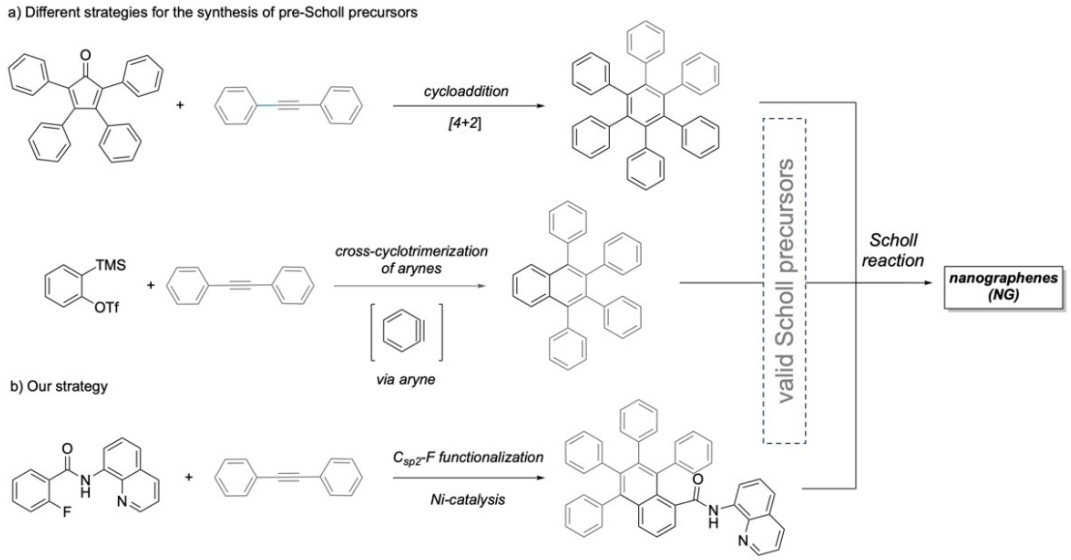

Figure 1. A) Reported strategies for the synthesis of NG precursors ([4 + 2] cycloaddition using cyclopentadienone and cross-cyclotrimerization of arynes depicted). B) Our strategy involving straightforward Ni-catalysed C_{sp2}–F activation for aromatic homologation as valid precursors of PAHs and NGs.

establish novel chemo- and regioselective transformation of fluorinated arenes for their productive degradation towards new useful PAH and NG materials.

Results and Discussion

We started our endeavour by taking advantage of the synthesis of aromatic homologation compounds via one-step Ni-catalysed C_{sp2}–F functionalization coupled with double insertion of diphenyl acetylenes. A more facile C_{sp2}–F over C_{sp2}–OMe functionalization was found in obtaining the aromatic homologation compounds **1a** and **1b** in good yields (63% and 44%, respectively).[16] Due to their facile synthesis, we took **1a** and **1b** as standard precursors for studying their ring-fusion in a variety of reported experimental conditions where we thoroughly analysed the nature of the oxidant and its concentration, the concentration of triflic acid and the reaction time. We previously reported that **1a** underwent double ring fusion along with hydrolysis and esterification of the AQ directing group.[16] We have revisited the experimental conditions and found that under 5.0 equivalents of chloranil as oxidant and 429 equiv. of triflic acid the doubly fused compound **2a** was obtained in 32% yield, where the AQ is left intact (Scheme 1). Similar conditions were applied to **1b** to obtain analogous methoxy-substituted **2b** in 36% yield. Both **2a** and **2b** are NGs possessing a decorated benzo[fg]naphtho[1,2,3-op]tetracene core, with interesting photophysical properties analysed later on.

Next, we analysed the effect of reducing the equivalents of triflic acid aiming at controlling the number of rings fused. To our surprise, under low triflic acid content (69 equiv. compared to 429 equiv.) and using DDQ as oxidant, **1a** was converted to a new compound **3a** in 37% yield at short reaction time (15 min) (Table 1, entry 1). Crystals of **3a** were obtained from a double layer diffusion of pentane into a concentrated solution of **3a** in

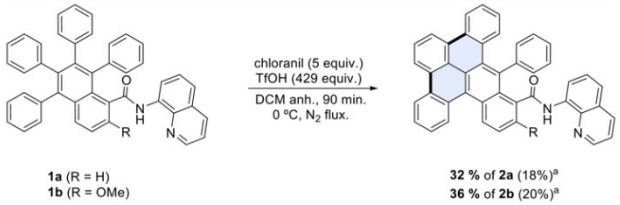

Scheme 1. Aromatic homologation compounds as basic models for the synthesis of NGs **2a** and **2b**.[a] Yield calculated from ^{1}H NMR of crude mixture using 1,3,5-trimethoxybenzene as internal standard (isolated yield in parenthesis).

Table 1. Synthesis of PAH bearing furanol cores, **3a**/**3b** and **4a**, using low triflic acid loadings.

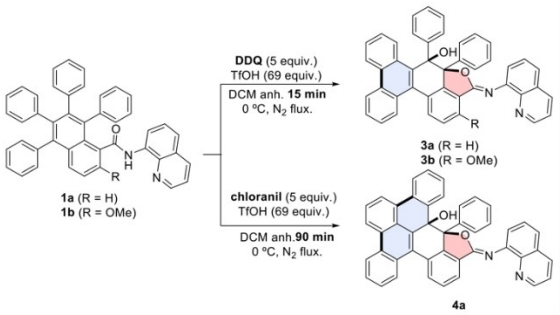

Entry[a]	1x	Oxidant	Time [min.]	Yield of 3a/3b [%][b]	Yield of 4a [%][b]
1	**1a**	DDQ	15	**37% of 3a (36%)**	–
2	**1b**	DDQ	15	**40% of 3b (28%)**	–
3[c]	**1a**	chloranil	90	–	**46% of 4a (37%)**

[a] Standard conditions: **1x** (0.033 mmol), oxidant (0.165 mmol), TfOH (0.2 mL), DCM (15 mL), N_2 flux, 0 °C. [b] Yield calculated from ^{1}H NMR of crude mixture using 1,3,5-trimethoxybenzene as internal standard (isolated yields in parenthesis). [c] 10% of **2a** was observed.

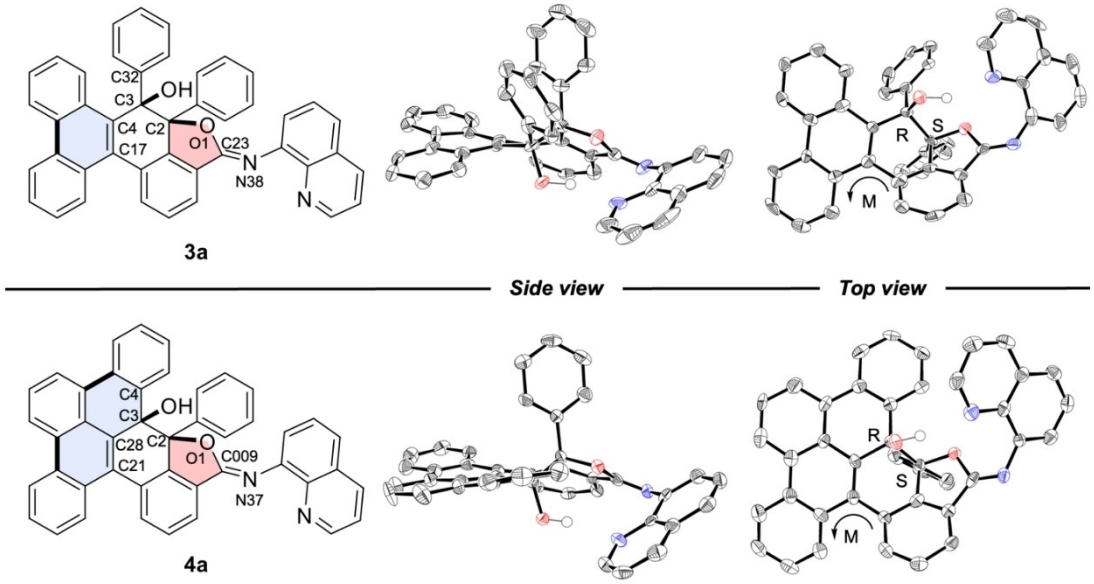

Figure 2. Crystal structure of PAH **3a** and **4a** (only (*M*)-(*R,S*)-enantiomer is shown, *R* chirality on the C*-OH and *S* chirality on the C*-Ofuran).

$CHCl_3$. Its crystal structure showed that the carbonyl moiety of the AQ directing group was integrated in the PAH structure featuring a 5a,6-diphenyl-5a,6-dihydro-4H-benzo[5,6]chryseno [12,1-bc]furan-6-ol core, thus with two aromatic rings fused (see Table 1). Analogously, the methoxy-derivative **3b** was obtained in 40% yield by submitting **1b** to the same experimental conditions.

At this point we focused on analysing the impact of the reaction outcome by using another oxidant. Indeed, using chloranil as oxidant (Table 1, entry 3) a new PAH, **4a** was formed in 46% yield. The solid-state structure showed an analogous structure as **3a** but with an additional ring fusion, thus featuring a 2a-phenyl-1,2a-dihydro-2bH-benzo[5,6]naphtho[1′,2′,3′,4′:12,1] tetrapheno[7,8-bc]furan-2b-ol core. By subjecting the methoxy-derivative **1b** to the same conditions, the corresponding **4b** product was not detected, instead, 31% of **2b** was observed.

A close analysis of the crystal structures of the PAH **3a** indicated that it consists of the racemic mixture of the (*M*)-(*R,S*)-**3a** and (*P*)-(*S,R*)-**3a** (Figure 2). Intrigued by this, the two enantiomers of **3a** were separated by chiral HPLC and analysed independently. The same racemic mixture was crystallised for **4a**, featuring (*M*)-(*R,S*)-**4a** and (*P*)-(*S,R*)-**4a** enantiomers in the crystal unit cell.

Comparing the two structures it can be observed some similitudes between them. The bond distances between C2–C3 are 1.589 Å and 1.587 Å in **3a** and **4a**, respectively, due to the dearomatization of the central ring. Moreover, the attack of the carbonyl group forming this furan-like ring causes the increase of the C23–O1 bond lengths to 1.373 Å in **3a**, and C009–O1 of 1.396 Å in **4a**. The formation of the C=N double bond is also observed with the short C23–N38 distance of 1.248 Å in **3a** and 1.255 Å (C009–N37) in **4a**. Moreover, the extended ring fused structure of **4a** compared to **3a** can be observed with the flattened torsion angle C21–C28–C3–C4 of 163.4° compared to 138.4° for the equivalent atoms (C17–C4–C3–C32) in **3a** (Figure 2).

Owing to the number of reported experimental conditions to date for the Scholl-type reaction, we explored the outcome of submitting our model PAH precursor **1a** to other methodologies. First, we explored using the $FeCl_3/MeNO_2$ conditions (instead of oxidant/TfOH) and gratifyingly a new compound **5a** was obtained in a good 70% isolated yield (Scheme 2). Compound **5a** was structurally characterized thoroughly, and its crystal structure showed the cleavage of the directing group and concomitant fusion of the carbonyl moiety into the final 1,2,3-triphenyl-7H- benzo[de]anthracen-7-one structure (Figure 3). The C2–C17 bond distance of 1.492 Å indicated the formation of a single bond. Moreover, the newly formed benzoanthracene scaffold showed a flattened torsion angle C13–C12–C11–C18 of 168.7°.

The analogous **5b** compound was also obtained in 80% isolated yield by treating **1b** to the same experimental conditions. The latter $FeCl_3/MeNO_2$ conditions to obtain **5a** stand as an orthogonal methodology to the DDQ/TfOH conditions because no aromatic ring fusion is obtained. Furthermore, no further ring fusion is obtained either by submitting **5a**/**5b** to DDQ/TfOH conditions presumably due to

Scheme 2. Synthesis of **5a** and **5b** upon reaction of **1a**/**1b** under $FeCl_3/MeNO_2$ conditions.

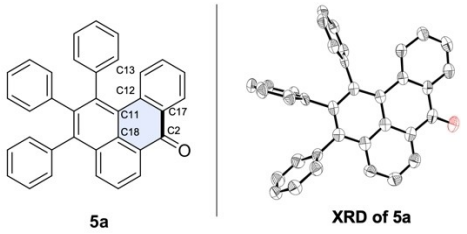

Figure 3. Crystal structure of the PAH **5a**.

the rigid planarity imposed by the formation of benzoanthracene moiety. In line with this hypothesis, when **2a** was subjected to $FeCl_3/MeNO_2$ conditions, the corresponding fused product was not detected (see Scheme S8).

Finally, Itami and Ito groups reported a novel mechanochemical (ball-milling) Li^0-based methodology for reductive ring fusion at room temperature and very short reaction times.[18] However, the reaction was not successful in our system and the starting material was fully recovered.

All compounds exhibited fluorescence emission, supported by the short emission lifetime values, in the order of a few nanoseconds and to the small Stokes' shift, and has been ascribed to π–π^* ^{1}IL transitions (Figure 4, Table 2 and Figures S52–S62). Aromatic homologation compounds **1a** and **1b** were almost not fluorescent ($\phi_{Fl}=0.01$ and 0.03, $\lambda_{em}=417$ and 405 nm, respectively), but the graphitized **2a** showed a remarkable 30-fold enhanced quantum yield and red shift of the emission maximum ($\phi_{Fl}=0.27$, $\lambda_{em}=474$ nm).

On the other hand, a modest 2-fold increase of quantum yield is obtained when a donating -OMe group is attached as in **2b** ($\phi_{Fl}=0.05$, $\lambda_{em}=495$ nm). On the other hand, and albeit furan-containing **3a** has a low quantum yield ($\phi_{Fl}=0.01$), its comparison to **4a** clearly shows that by extending the fused-ring π-system the quantum yield increases by 6-fold up to ($\phi_{Fl}=$ 0.07). Remarkably, the benzo-anthracenone derivative **5a** is highly fluorescent in MeOH ($\phi_{Fl}=0.63$, $\lambda_{em}=512$ nm) but severely quenched in CH_2Cl_2 ($\phi_{Fl}=0.04$, $\lambda_{em}=485$ nm).[19] On the other hand, the fluorescence of the methoxy analogue **5b** in MeOH is severely quenched ($\phi_{Fl}=0.02$, $\lambda_{em}=490$ nm).

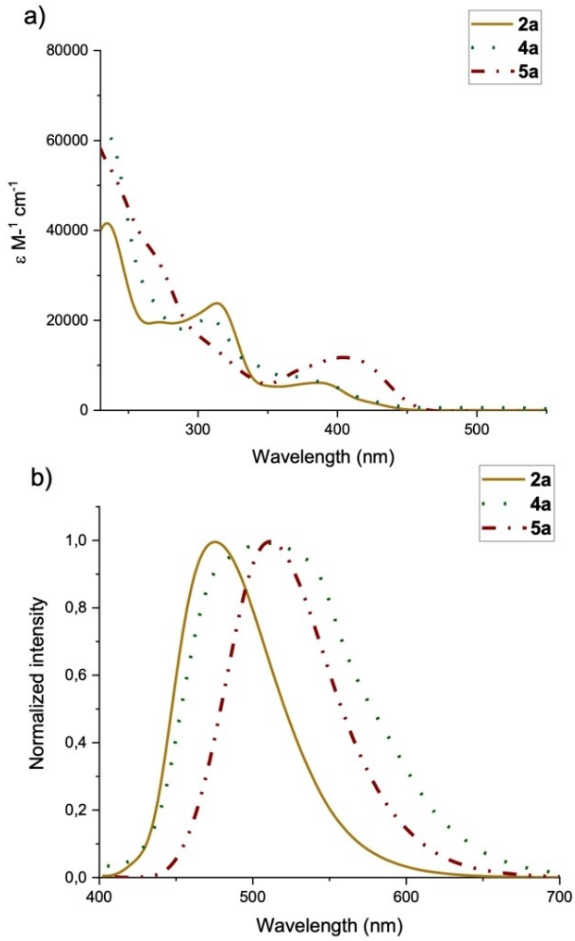

Figure 4. a) UV/Vis absorption spectra of **2a**, **4a** in CH_2Cl_2 and **5a** in MeOH at 1×10^{-5} M. (b) Normalized emission spectra of **2a**, **4a** in CH_2Cl_2 and **5a** in MeOH at 1×10^{-5} M.

The chiral resolution of **3a** was achieved using high-performance liquid chromatography (HPLC). The well-separated fractions F1 and F2 (using the CHIRALPAK® IC column) were collected (Figure 5A) and the chiroptical properties of each isomer were analysed by circular dichroism (CD) (Figure 5B). Enantiomerically pure F1 and F2 fractions exhibit mirror-image

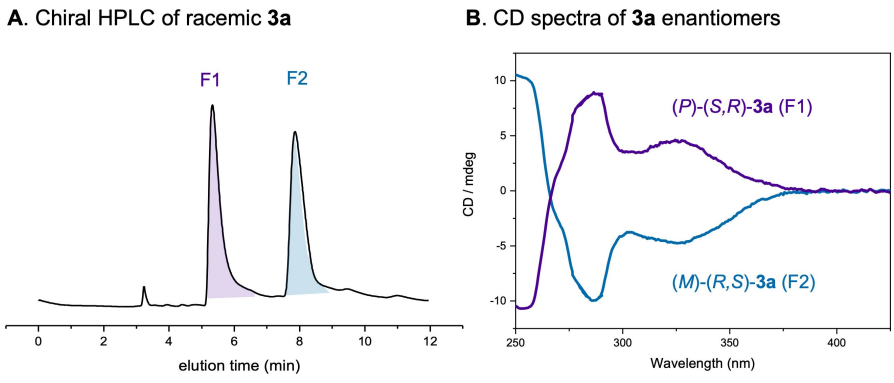

Figure 5. a) Chiral HPLC chromatogram of **3a** racemic mixture. b) Experimental CD spectra of the two enantiomers *(P)-(S,R)*-**3a** (3×10^{-4} M) and *(M)-(R,S)*-**3a** (1×10^{-5} M) in CH_2Cl_2.

Table 2. Absorption and emission data, luminescence quantum yield and lifetimes measured for all compounds in CH_2Cl_2 at 10^{-5} M.

Entry	Compound	λ_{abs} [nm] ε[10^4 $M^{-1}cm^{-1}$]	λ_{em} [nm]	Φ_{FI}	τ [ns]
1	1a	318 (1.3) 325 (1.3)	417	0.01	<1
2	1b	310 (1.8) 343 (1.5)	405	0.03	<1
3	2a	317 (2.3) 392 (0.6)	474	0.27	2.20
4	2b	317 (6.8) 378 (1.3)	495	0.05	<1
5	3a	331 (1.6)	476	0.01	4.51
6	3b	333 (1.3)	437	0.01	<1
7	4a	314 (2.3) 495 (0.6)	507	0.07	2.23
8	5a	380 (1.6) 400 (1.8)	485	0.04	<1
9[a]	5a	404 (1.3)	512	0.63	8.92
10	5b	366 (3.1)	470	0.00	<1
11[a]	5b	368 (1.0)	490	0.02	<1

[a] measured in MeOH at $1\cdot10^{-5}$ M.

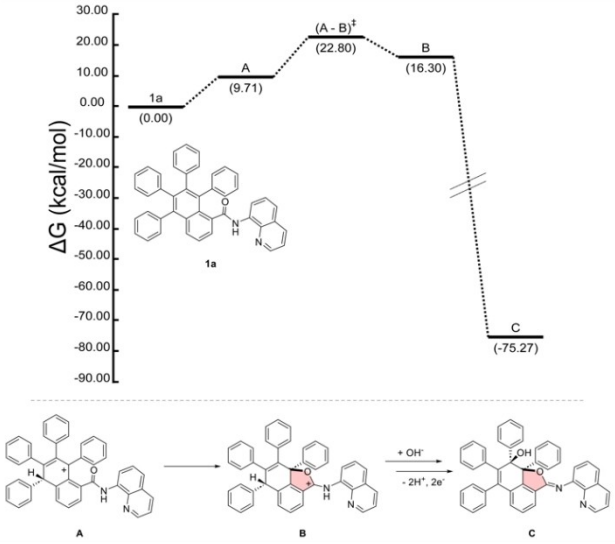

Figure 6. Proposed reaction mechanism and Gibbs free-energy diagram of the formation of the furan ring.

CD spectra with negative and positive peaks at 255, 289 and 330 nm. The comparison with TD-DFT simulations of *(M)-(R,S)*-**3a** (see Figure S73) allowed the assignment of this enantiomer to F2, and therefore F1 fraction corresponded to *(P)-(S,R)*-**3a**. The absorption dissymmetry factor (g_{abs}) of *(P)-(S,R)*-**3a** and *(M)-(R,S)*-**3a** at 289 nm is 2.8×10^{-5} and -9.2×10^{-4} respectively.

The origin of the furan-6-ol derivatives **3a** and **4a** was intriguing. A thorough DFT analysis was conducted to shed light on their mechanism of formation (B3LYP-D3/6-311G(d) level with the SMD continuum solvent model for CH_2Cl_2). Both arenium ion pathway and radical cation pathway for the Scholl reaction were computed, being the arenium pathway energetically favourable in all ring fusions studied (see Section 9 in Supporting Information), as observed in previous studies.[20] Following the arenium mechanism, the first protonation at the central naphthalene-ring generates an energetically accessible carbocation stabilised at a benzylic position that triggers the furan-cyclization by the carbonyl moiety of the amide directing group, with a low barrier (**A**→**B**, $\Delta G^{\ddagger}_{DCM=}$13.1 kcal/mol, Figure 6). Subsequent oxidation and deprotonation steps allow the formation first of the alcohol by OH^- attack and the concomitant reorganization leading to the formation of ((Z)-6,7,8,8a-tetraphenyl-2-(quinolin-8-ylimino)-8,8a-dihydro-2H naphtho[1,8-bc]furan-8-ol product (**C**). The latter is not trapped experimentally because competing ring fusion takes place, and either **3a** (two-ring fusion) or **4a** (three-ring fusion) are obtained. DFT analysis indicates that after protonation of **C**, a low barrier of 15.9 kcal/mol from **D**→**E** (Figure 7) allows the formation of the two-ring fused product **3a**. Subsequent protonation of **3a** affords species **F**, which undergoes ulterior ring fusion to finally form **4a** with a barrier of $\Delta G^{\ddagger}_{DCM}$ = 15.3 kcal/mol.

Ring fusion process, after furan formation, is more favourable than direct ring fusion from **1a** ($\Delta G^{\ddagger}_{DCM}$ = 21.3 kcal/mol, Figure S69). This higher energy barrier for ring fusion in the absence of furan formation indicates that furan cyclization occurs prior to ring fusions (Figure S70). In line with this

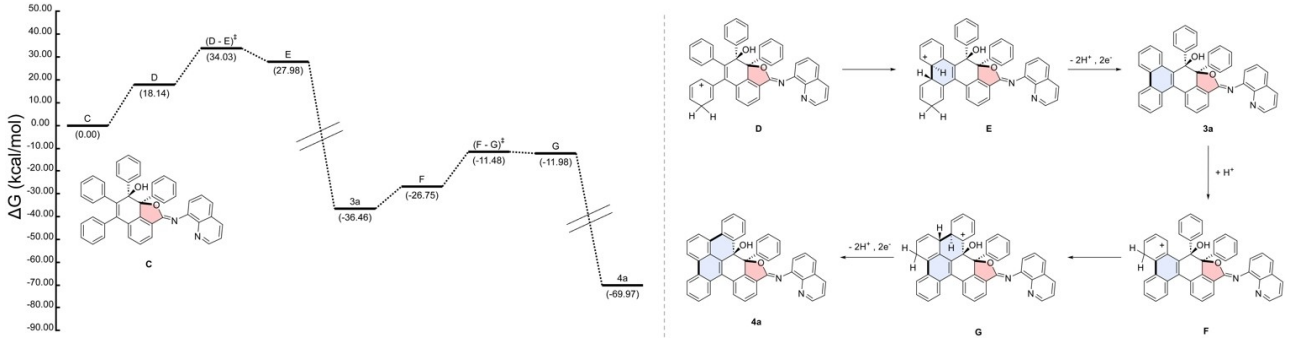

Figure 7. Proposed reaction mechanism and Gibbs free-energy diagram of the stepwise ring fusions towards **3a** and **4a**.

hypothesis, by submitting compound **2a** (featuring 3 fused rings) to the specific experimental conditions for furan-ring formation, only traces of **4a** were detected.

Experimentally, strong acidic conditions (TfOH/oxidant ratio >85) preclude furan formation and only three-ring fused product **2a** is obtained (Scheme 1). On the contrary, under significantly less acidic conditions (TfOH/oxidant ratio <14), only the furan-ring products **3a** and **4a** are obtained (Table 1). We hypothesized that protonation of carbonyl moiety of the aminoquinoline moiety of **1a** precludes the furan ring formation. Hence, upon protonation of the carbonyl, a feasible energy barrier of 20.6 kcal/mol to finally produce the ring fused **2a** is obtained (Figure S72). Indeed, lowering the pH implies fewer OH^- anions available for the formation of benzo-chryseno-furanol species **3a**. Nonetheless, the location of the initial protonation site is related to the aromaticity of the different rings in **1a**. Phenyl groups are more aromatic than naphthalene, therefore, when a phenyl moiety is protonated the destabilization (dearomatization) is larger ($\Delta_{MCI}=0.060$) than in the naphthalene ring ($\Delta_{MCI}=0.028$) (Figure 8). Thus, the latter is also in line with the preferential naphthalene protonation to tigger the furan formation prior to ring fusions under moderately acidic conditions.

Conclusions

In summary, we have reported the stepwise synthesis of new NGs and PAHs obtained via Scholl ring fusion applied at aromatic homologation compounds, which are obtained through one-step Ni-catalysed C_{sp2}–F functionalization. The easy access to valid Scholl precursors allowed us to obtain a variety of NGs and PAHs and to gain detailed experimental and theoretical mechanistic information on this highly unpredictable reaction, especially on the formation of the furanol PAHs **3a** and **4a** under moderately acidic conditions. The furanol-bearing PAHs represent a snapshot to new Scholl reaction pathways, and proof that necessary DG in the synthesis of the precursors can be used as a handle to produce structural diversity. Importantly, DFT studies allowed us to rationalize the formation of the furanol ring prior to ring fusions, and also provided a feasible protonation-oxidative ring fusion sequence for the formation of the PAHs. Indeed, we are currently exploring further derivatization of the PAHs reported.

Moreover, the fluorescent properties and quantum yields are reported for all compounds described, showing a rational control of the luminescent properties depending on ring fusions. In the case of racemic furanol **3a**, enantiomeric separation by chiral HPLC allowed the study of their chiroptical CD properties. Our team is currently investigating the synthesis of other Ni-catalysed aromatic homologation precursors to expand the family of (hetero)NGs using our bottom-up stepwise strategy.

Experimental Section

See Supporting Information for materials, instrumentation, experimental procedures, spectroscopic and photophysical characterization of all compounds.

Deposition Number(s) 2285382 (**3a**), 2285383 (**4a**), 2285384 (**5a**) contain(s) the supplementary crystallographic data for this paper. These data are provided free of charge by the joint Cambridge Crystallographic Data Centre and Fachinformationszentrum Karlsruhe Access Structures service.

Acknowledgements

This work was financially supported by grants from MINECO-Spain (PID2019-104498GB-I00, PID2022-136970NB-I00 and TED2021-130573B-I00 to X.R., PID2020-113711GB-100 to S.S, PID2019-104121GB-I00 to L.R.), and Generalitat de Catalunya (2021SGR00475 and ICREA Academia to X.R.). J.S. thanks GenCat for a PhD FI grant. We also thank funding from Red de Investigación OASIS (RED2022-134074-T).

Conflict of Interests

The authors declare no conflict of interest.

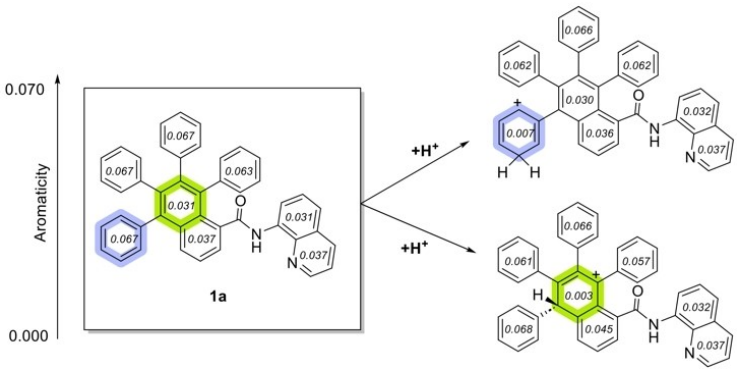

Figure 8. Aromaticity (MCI values) of **1a** and corresponding dearomatization of the protonated species at phenyl or naphthalene rings.

Data Availability Statement

The data that support the findings of this study are available in the supplementary material of this article.

Keywords: chiral PAH · DFT · nanographenes · nickel catalysis · Scholl reaction

[1] a) J. Wagner, P. Zimmermann Crocomo, M. A. Kochman, A. Kubas, P. Data, M. Lindner, *Angew. Chem. Int. Ed.* **2022**, *61*, e202202232; b) C. Zong, X. Zhu, Z. Xu, L. Zhang, J. Xu, J. Guo, Q. Xiang, Z. Zeng, W. Hu, J. Wu, R. Li, Z. Sun, *Angew. Chem. Int. Ed.* **2021**, *60*, 16230–16236; *Angew. Chem.* **2021**, *133*, 16366–16372.
[2] Y. Gu, Z. Qiu, K. Müllen, *J. Am. Chem. Soc.* **2022**, *144*, 11499–11524.
[3] a) J. Han, S. Guo, H. Lu, S. Liu, Q. Zhao, W. Huang, *Adv. Opt. Mater.* **2018**, *6*, 1800538; b) J. M. Fernández-García, P. Izquierdo-García, M. Buendía, S. Filippone, N. Martín, *Chem. Commun.* **2022**, *58*, 2634–2645; c) Y.-J. Shen, N.-T. Yao, L.-N. Diao, Y. Yang, X.-L. Chen, H.-Y. Gong, *Angew. Chem. Int. Ed.* **2023**, *62*, e202300840; *Angew. Chem.* **2023**, *135*, e202300840; d) J. Wang, C. Shen, G. Zhang, F. Gan, Y. Ding, H. Qiu, *Angew. Chem. Int. Ed.* **2022**, *61*, e202115979; *Angew. Chem.* **2022**, *134*, e202115979.
[4] A. Narita, X.-Y. Wang, X. Feng, K. Müllen, *Chem. Soc. Rev.* **2015**, *44*, 6616–6643.
[5] M. Rickhaus, M. Mayor, M. Juríček, *Chem. Soc. Rev.* **2016**, *45*, 1542–1556.
[6] R. Balog, B. Jørgensen, L. Nilsson, M. Andersen, E. Rienks, M. Bianchi, M. Fanetti, E. Lægsgaard, A. Baraldi, S. Lizzit, Z. Sljivancanin, F. Besenbacher, B. Hammer, T. G. Pedersen, P. Hofmann, L. Hornekær, *Nat. Mater.* **2010**, *9*, 315–319.
[7] a) J. Urieta-Mora, I. García-Benito, A. Molina-Ontoria, N. Martín, *Chem. Soc. Rev.* **2018**, *47*, 8541–8571; b) S. Zank, J. M. Fernández-García, A. J. Stasyuk, A. A. Voityuk, M. Krug, M. Solà, D. M. Guldi, N. Martín, *Angew. Chem. Int. Ed.* **2022**, *61*, e202112834; *Angew. Chem.* **2022**, *134*, e202112834; c) N. Panwar, A. M. Soehartono, K. K. Chan, S. Zeng, G. Xu, J. Qu, P. Coquet, K.-T. Yong, X. Chen, *Chem. Rev.* **2019**, *119*, 9559–9656; d) S. Míguez-Lago, I. F. A. Mariz, M. A. Medel, J. M. Cuerva, E. Maçôas, C. M. Cruz, A. G. Campaña, *Chem. Sci.* **2022**, *13*, 10267–10272; e) J.-K. Li, X.-Y. Chen, W.-L. Zhao, Y.-L. Guo, Y. Zhang, X.-C. Wang, A. C.-H. Sue, X.-Y. Cao, M. Li, C.-F. Chen, X.-Y. Wang, *Angew. Chem. Int. Ed.* **2023**, *62*, e202215367; *Angew. Chem.* **2023**, *135*, e202215367.
[8] S. Fujii, T. Enoki, *Acc. Chem. Res.* **2013**, *46*, 2202–2210.
[9] a) P. Izquierdo-García, J. M. Fernández-García, J. Perles, I. Fernández, N. Martín, *Angew. Chem. Int. Ed.* **2023**, *62*, e202215655; *Angew. Chem.* **2023**, *135*, e202215655; b) R. Scholl, C. Seer, *Justus Liebigs Ann. Chem.* **1912**, *394*, 111–177; c) M. Grzybowski, B. Sadowski, H. Butenschön, D. T. Gryko, *Angew. Chem. Int. Ed.* **2020**, *59*, 2998–3027; *Angew. Chem.* **2020**, *132*, 3020–3050.
[10] P. K. Sharma, A. Babbar, D. Mallick, S. Das, *J. Org. Chem.* **2023**, *88*, 5473–5482.
[11] a) W. Hagui, H. Doucet, J.-F. Soulé, *Chem* **2019**, *5*, 2006–2078; b) D. Lungerich, D. Reger, H. Hölzel, R. Riedel, M. M. J. C. Martin, F. Hampel, N. Jux, *Angew. Chem. Int. Ed.* **2016**, *55*, 5602–5605; *Angew. Chem.* **2016**, *128*, 5692–5696.
[12] a) H. Ito, Y. Segawa, K. Murakami, K. Itami, *J. Am. Chem. Soc.* **2019**, *141*, 3–10; b) K. P. Kawahara, W. Matsuoka, H. Ito, K. Itami, *Angew. Chem. Int. Ed.* **2020**, *59*, 6383–6388; *Angew. Chem.* **2020**, *132*, 6445–6450.
[13] a) I. Pozo, E. Guitián, D. Pérez, D. Peña, *Acc. Chem. Res.* **2019**, *52*, 2472–2481; b) A. Yubuta, T. Hosokawa, M. Gon, K. Tanaka, Y. Chujo, A. Tsurusaki, K. Kamikawa, *J. Am. Chem. Soc.* **2020**, *142*, 10025–10033.
[14] a) Q. Miao, *Nat. Chem. Rev.* **2021**, *5*, 602–603; b) J. Liu, A. Narita, S. Osella, W. Zhang, D. Schollmeyer, D. Beljonne, X. Feng, K. Müllen, *J. Am. Chem. Soc.* **2016**, *138*, 2602–2608; c) G. González Miera, S. Matsubara, H. Kono, K. Murakami, K. Itami, *Chem. Sci.* **2022**, *13*, 1848–1868.
[15] L. Capdevila, T. H. Meyer, S. Roldán-Gómez, J. M. Luis, L. Ackermann, X. Ribas, *ACS Catal.* **2019**, *9*, 11074–11081.
[16] L. Capdevila, J. Sala, L. Ackermann, X. Ribas, *Chem. Eur. J.* **2022**, *28*, e202200625.
[17] a) Y. Zhang, S. H. Pun, Q. Miao, *Chem. Rev.* **2022**, *122*, 14554–14593; b) H. V. Anderson, N. D. Gois, W. A. Chalifoux, *Org. Chem. Front.* **2023**, *10*, 4167–4197; c) N. Ponugoti, V. Parthasarathy, *Chem. Eur. J.* **2022**, *28*, e202103530.
[18] K. Fujishiro, Y. Morinaka, Y. Ono, T. Tanaka, L. T. Scott, H. Ito, K. Itami, *J. Am. Chem. Soc.* **2023**, *145*, 8163–8175.
[19] a) J. P. Kurtz, T. Grusenmeyer, L. Tong, G. Kosgei, R. H. Schmehl, J. T. Mague, R. A. Pascal, *Tetrahedron* **2011**, *67*, 7211–7216; b) H. Chen, L. Ouyang, J. Liu, W.-J. Shi, G. Chen, L. Zheng, *J. Org. Chem.* **2019**, *84*, 12755–12763.
[20] a) P. Rempala, J. Kroulík, B. T. King, *J. Org. Chem.* **2006**, *71*, 5067–5081; b) B. T. King, J. Kroulík, C. R. Robertson, P. Rempala, C. L. Hilton, J. D. Korinek, L. M. Gortari, *J. Org. Chem.* **2007**, *72*, 2279–2288; c) L. Zhai, R. Shukla, S. H. Wadumethrige, R. Rathore, *J. Org. Chem.* **2010**, *75*, 4748–4760; d) C. Shen, G. Zhang, Y. Ding, N. Yang, F. Gan, J. Crassous, H. Qiu, *Nat. Commun.* **2021**, *12*, 2786; e) Y. Zou, Y. Han, S. Wu, X. Hou, C. H. E. Chow, J. Wu, *Angew. Chem. Int. Ed.* **2021**, *60*, 17654–17663; *Angew. Chem.* **2021**, *133*, 17795–17804.

Manuscript received: September 30, 2023
Accepted manuscript online: October 30, 2023
Version of record online: December 6, 2023